Journal of Cerebral Blood Flow & Metabolism (2013) 33, 356–364

www.jcbfm.com

ORIGINAL ARTICLE

Glibenclamide enhances neurogenesis and improves long-term functional recovery after transient focal cerebral ischemia

Francisco J Ortega[1,2], Jukka Jolkkonen[2], Nicole Mahy[1] and Manuel J Rodríguez[1]

Glibenclamide is neuroprotective against cerebral ischemia in rats. We studied whether glibenclamide enhances long-term brain repair and improves behavioral recovery after stroke. Adult male Wistar rats were subjected to transient middle cerebral artery occlusion (MCAO) for 90 minutes. A low dose of glibenclamide (total 0.6 μg) was administered intravenously 6, 12, and 24 hours after reperfusion. We assessed behavioral outcome during a 30-day follow-up and animals were perfused for histological evaluation. *In vitro* specific binding of glibenclamide to microglia increased after pro-inflammatory stimuli. *In vivo* glibenclamide was associated with increased migration of doublecortin-positive cells in the striatum toward the ischemic lesion 72 hours after MCAO, and reactive microglia expressed sulfonylurea receptor 1 (SUR1) and Kir6.2 in the medial striatum. One month after MCAO, glibenclamide was also associated with increased number of NeuN-positive and 5-bromo-2-deoxyuridine-positive neurons in the cortex and hippocampus, and enhanced angiogenesis in the hippocampus. Consequently, glibenclamide-treated MCAO rats showed improved performance in the limb-placing test on postoperative days 22 to 29, and in the cylinder and water-maze test on postoperative day 29. Therefore, acute blockade of SUR1 by glibenclamide enhanced long-term brain repair in MCAO rats, which was associated with improved behavioral outcome.

Journal of Cerebral Blood Flow & Metabolism (2013) **33,** 356–364; doi:10.1038/jcbfm.2012.166; published online 14 November 2012

Keywords: angiogenesis; brain ischemia; microglia; neural stem cells; neuroprotection; regeneration and recovery

INTRODUCTION

The therapeutic potential of the administration of low doses of glibenclamide has been confirmed in different central nervous system pathologies.[1] In experimental stroke models it reduces cerebral edema and infarct volume, and decreases mortality.[2,3] In addition, this has been confirmed in stroke patients, where a retrospective study found that patients with diabetes mellitus taking glibenclamide that suffered an acute ischemic stroke had a better neurological outcome.[4]

Glibenclamide blocks the sulfonylurea receptor 1 (SUR1), the regulatory subunit of the K_{ATP}[5] and the $NC_{Ca\text{-}ATP}$ channels,[1,6] which under ischemic conditions are expressed in neurons, astrocytes, oligodendrocytes, endothelial cells,[1,7] and by reactive microglia.[8] It has been proposed that the blockade of the astroglial $NC_{Ca\text{-}ATP}$ channel by glibenclamide prevents cytotoxic edema after cerebral ischemia.[1,7] However, glibenclamide administration resulted in ameliorated reperfusion-derived oxidative stress and pro-inflammatory cytokine release in the rat hippocampus after cerebral ischemia in rats.[9] In line with this, our previous study demonstrated that glibenclamide administration at 6, 12, and 24 hours after reperfusion caused early neuroprotection and this was accompanied by a better neurological outcome.[8] Although recently Simard *et al*[10] showed an extended time window for glibenclamide treatment from 6 to 10 hours after onset of cerebral ischemia, and several studies point to a beneficial effect of glibenclamide to treat stroke, no previous studies have evaluated the long-term effects of glibenclamide administration on brain repair and its correlation with functional outcomes after stroke.

Our previous studies also showed that reactive microglia increase their expression of the K_{ATP}-channel components Kir6.1, Kir6.2, SUR1, and SUR2B after brain pathologies, and the *in vitro* pharmacology of the K_{ATP}-channel open state regulates the release of cytokines.[8,11,12] More precisely, glibenclamide increased the reactive morphology, phagocytic capacity, and tumor necrosis factor-α secretion of reactive microglia *in vitro*. Thus, as cerebral ischemia leads to an accumulation of microglia in the sub-ventricular zone, from where newly formed neuroblasts migrate toward the ischemic boundary zone,[13] is likely that controlling the phenotype of activated microglia will promote brain repair. This will provide neuroprotection[14] and pro-neurogenic mediators that support the different steps of neurogenesis.[15,16] Indeed, stroke induces cortical neurogenesis in animals models[17,18] and, more importantly, in the adult human brain.[19,20] Whether microglia influence these processes and the fate of the newborn neurons

[1]Unitat de Bioquímica i Biologia Molecular, the Facultat de Medicina, the Institut d'Investigacions Biomèdiques August Pi i Sunyer (IDIBAPS), the Universitat de Barcelona and the Centro de Investigación Biomédica en Red sobre Enfermedades Neurodegenerativas (CIBERNED), Barcelona, Spain and [2]Institute of Clinical Medicine – Neurology, University of Eastern Finland, Kuopio, Finland. Correspondence: Dr FJ Ortega, Unitat de Bioquímica i Biologia Molecular, Facultat de Medicina, the Institut d'Investigacions Biomèdiques August Pi i Sunyer (IDIBAPS), the Universitat de Barcelona and the Centro de Investigación Biomédica en Red sobre Enfermedades Neurodegenerativas (CIBERNED), UB, c/ Casanova 143, Barcelona E-08036, Spain.
E-mail: j.ortega@ub.edu

We thank Nanna Huuskonen, Laura Tolppanen, Anu Lipsanen, and Dr Tony Valente for their invaluable expert technical help. This work was supported by grants SAF2008-01902 from the Ministerio de Ciencia e Innovación, and by grant 2009SGR1380 from the Generalitat de Catalunya (Autonomous Government), Spain; and Center for International Mobility (CIMO), Finland. FJO held a fellowship from Spanish Ministerio de Educación.
Received 26 June 2012; revised 12 October 2012; accepted 18 October 2012; published online 14 November 2012

is still unclear. Nonetheless, although there is contradictory evidence for microglia being pro-neurogenic, several recent findings reinforce the hypothesis that microglia can direct neurogenesis.[16,21]

We hypothesized that early blockade of SUR1 by glibenclamide after cerebral ischemia enhances ischemia-induced neurogenesis in the striatum and long-term brain repair, thus leading to an improved functional outcome. To test this hypothesis, we treated rats with low doses of glibenclamide intravenously early after focal cerebral ischemia and evaluated long-term neuroprotection, neurogenesis, angiogenesis, and behavioral recovery. Next, to assess whether microglia could be involved in neurogenesis, we analyzed the expression *in vivo* of SUR1 by reactive microglia after ischemia and whether glibenclamide binds specifically to microglia using primary rat microglia cultures.

METHODS

Transient occlusion of the middle cerebral artery in rats

Male Wistar rats (3 months old and weighing 250–300 g at the beginning of the study; National Laboratory Animal Center, Kuopio, Finland) were used. They were kept on a 12/12 hours day and night cycle and housed individually with free access to food and water ($20 \pm 1\ ^{\circ}C$). Animals were handled following European legislation (86/609/EEC) and all efforts were made to minimize the number used and animal suffering, in accordance with the ARRIVE guidelines. The Animal Ethics Committee (Hämeenlinna, Finland) approved the study.

Focal cerebral ischemia was induced by the intraluminal filament technique as described elsewhere.[8] Briefly, the rats were anesthetized with 5% halothane (in 70% N_2O/30% O_2) and a surgical depth of anesthesia was maintained throughout the operation with 0.5 to 1% halothane delivered though a nose mask. The right common carotid artery was exposed through a midline cervical incision under a surgical microscope and gently separated from the nerves. A heparinized nylon filament (diameter 0.25 mm, rounded tip) was inserted into the stump of the external common carotid artery and advanced into the internal carotid artery 1.8–2.1 cm until it blocked the blood flow into the middle cerebral artery. Corticostriatal damage was induced by an occlusion of the middle cerebral artery (MCAO) of 90 minutes and the blood flow was then restored by removing the filament. Sham-operated control rats underwent the same procedure except that the filament was not inserted. To balance the MCAO groups, the neurological symptoms were assessed before drug administration using two tests: contralateral rotation/circling behavior and impaired contralateral forelimb/hindlimb response to proprioceptive stimulus (i.e., lack of limb withdrawal when hanging over the edge of a table). Animals with no behavioral impairment were excluded from the study.

Drug treatment

We divided 34 rats into the following three groups: sham-operated rats ($n = 10$), vehicle-treated MCAO rats ($n = 12$), and glibenclamide-treated MCAO rats ($n = 12$). Rats were placed in a restrainer for drug administration in the distal portion of the vein. Each rat received three injections of 0.2 mL of either 0.01 mol/L phosphate-buffered saline (PBS; pH 7.4) or 0.2 μg glibenclamide into the tail vein 6, 12, and 24 hours after reperfusion (total dose 0.6 μg). Glibenclamide was prepared in dimethyl sulfoxide and diluted in 0.01 mol/L PBS to final concentration (dimethyl sulfoxide final concentration $< 0.5\%$). To analyze cell proliferation, we administered intraperitoneal injections of 5-bromo-2-deoxyuridine (BrdU) (50 mg/kg), with some modifications, as described elsewhere.[22] In summary, all rats received a single injection of BrdU daily from postoperative days 4 to 8. Infarct volumes were measured at the end of the study and unsuccessful transient MCAO animals were excluded from the study ($n = 2$ from vehicle group).

Behavioral outcome measures

Limb-placing test. The modified version of the limb-placing test[23] was performed before operation and on postoperative days 2, 4, 7, 10, 13, 16, 19, 22, 26, and 29. The animals were habituated for handling and testing before the induction of ischemia. The test included seven limb-placing tasks to assess the integration of forelimb and hindlimb responses to tactile and proprioceptive stimulation. Briefly, animals were placed on the edge of a table, and their forelimbs and hindlimbs were pushed over the edge to measure ability to retrieve their limbs. Tasks were performed from the front and the side of the rat, with and without the help of whisker stimuli. In addition, forelimb flexion was evaluated when the rat was lifted in the air by the base of its tail, and finally forepaw resistance was noted when the rat was pushed on the table surface. Both sides of the body were tested to assess forelimb and hindlimb function. An observer blind to the experimental groups performed the behavioral analysis. Scoring: 2 points, normal response; 1 point, delayed and/or incomplete response; 0 points, no response.

Forelimb asymmetry test. The cylinder test was used to assess imbalance between impaired and non-impaired forelimbs.[24] Briefly, the rats were placed in a Plexiglas cylinder (Ø 20 cm) for at least 4 minutes or until the rats were observed to rear a minimum of 20 times. Sessions were videotaped from below the cylinder and analyzed using a slow motion video recorder to determine the number of contacts by both forelimbs and by either impaired or non-impaired forelimbs. An observer blind to the experimental groups performed the behavioral analysis. The cylinder score for an impaired forelimb was calculated as: contralateral contacts/total contacts $\times$ 100%.

Tapered/ledged beam-walking test. The sensorimotor function of hindlimbs was evaluated using a tapered/ledged beam.[25] The beam-walking apparatus consisted of a tapered beam with underhanging ledges on each side to permit foot faults without falling and the end of the beam was connected to a black box. Steps onto the ledge were scored as a full slip and a half-slip was scored when the limb touched the side of the beam. The mean of three trials was used for statistical analyses. An observer blind to the experimental groups performed the behavioral analysis. Pretrained animals were tested in baseline conditions and on postoperative days 7 and 29. Performance was videotaped and analyzed by calculating the slip ratio as: [(full slips $+ 1/2 \times$ half slips)/total steps] $\times$ 100%.

Morris water-maze. Spatial learning was assessed using a modified version of the Morris water-maze task.[23] Rats were given four trials per day on postoperative days 26 to 28 followed by the probe trial without the platform. The pool (Ø 150 cm) was divided into four quadrants or three annulus zones of equal surface area. Starting locations were called north, south, east, and west, and were located arbitrarily at equal distances along the pool rim. The platform was located in the middle of the northeast quadrant 25 cm from the pool rim. When the rat failed to find the hidden platform within 50 seconds, it was placed on the platform. The animal was allowed to remain on the platform for 10 seconds and to rest for 1 minute after trials. The starting point was changed after each trial. The swim paths were monitored by a video camera connected to a computer through an image analyzer (HVS Image, Mountain View, CA, USA). Escape latency (time to reach the platform) and the path length the animal swam to find the platform were parameters used to assess their performance in the water-maze task. Swimming speed (path length/escape latency) was calculated to exclude the effect of sensorimotor impairment. At the end of the third testing day, a 30-second probe trial without the platform was used to evaluate how well rats remembered the location of the platform (passes over the previous platform location). An observer blind to the experimental groups performed the behavioral analysis. Time spent in different annulus zones and quadrants of the pool was analyzed to examine the search strategies used by the animals.

Immunohistochemistry

Thirty days after MCAO, rats were anesthetized and transcardially perfused with saline for 5 minutes, followed by 4% w/v paraformaldehyde in phosphate buffer. Brains were post-fixed, cryopreserved in 30% w/v sucrose, and frozen on dry ice. Sections (14 μm) covering the entire brain were cut with a cryotome.

The first section between bregma $+1.7$ and $+2.2$ of each animal stained with standard hematoxylin–eosin was selected at random. Sequential sections separated by 1 mm were selected for each animal to determine the total infarct volume using the optical microscope software AxioVision 4 AC (Zeiss, GmbH, Jena, Germany) and applying the Cavalieri's principle. This consisted of multiplying the infarct area by the distance between sections (1 mm) and combining the values from each section (5–6 sections/animal). The total infarct volume was calculated by subtracting the area of the remaining tissue in the ischemic hemisphere from the area of the intact contralateral tissue of each section.[23]

Immunohistochemistry was carried out with the avidin–biotin peroxidase method as previously described.[8] We used primary antibodies against doublecortin (DCX; clone C-18; 1:150; Santa Cruz, Santa Cruz, CA, USA) to detect undifferentiated neurons and NeuN (1:150; Chemicon, Temecula, CA, USA), calbindin (CB; 1:500; Swant, Bellinzona, Switzerland), parvalbumin (PV; 1:2000; Swant), tyrosine hydroxylase (TH; 1:5000; Abcam, Cambridge, UK), or calretinin (CR; 1:2000; Swant) for differentiated neurons.[26] To detect blood vessels, we used RECA-1 (1:100; Serotec, Oxford, UK). For glial detection, we used antibodies against GFAP (1:400; Sigma-Aldrich, St Louis, MO, USA), CD11b (OX-42 clone; 1:150; Serotec), or the isolectin B4 peroxidase-conjugated (IB4) from *Bandeiraea simplicifolia* (1:25; Sigma-Aldrich). We used an antibody against the sulfonylurea receptor 1 (SUR1; 1:100, Santa Cruz) to detect the glibenclamide target in microglial cells. The fate of the new proliferating cells was determined by double immunostaining with mouse monoclonal anti-BrdU antibody (1:100; Sigma-Aldrich) and biotin-conjugated rat antimouse IgG (1:150), and antibodies against specific cellular markers, as described elsewhere.[26] ExtrAvidin-FITC (1:250; Sigma-Adrich) was used to detect BrdU-positive cells. Also, for immunofluorescence we used primary antibodies against NeuN (1:150; Chemicon), GFAP (1:400; Sigma-Aldrich), CD11b (OX-42 clone; 1:150; Serotec), and caspase-3 (clone 5A1E; 1:500; Cell Signaling, Danvers, MA, USA). Then we used specific anti-IgGs conjugated with AlexaFluo-488 (1:300; Invitrogen, Carlsbad, CA, USA) to detect caspase-3 and specific anti-IgGs from various species conjugated with AlexaFluo-555 (1:300; Invitrogen) for the other cellular markers. Confocal images were acquired using a Leica TCS SL laser scanning confocal spectral microscope (Leica Microsystems Heidelberg GmbH, Mannheim, Germany) and images were analyzed with ImageJ 1.39 u (NIH, USA).

Degenerating neurons were detected by Fluoro-Jade B (FJB, Chemicon) fluorochrome, following the manufacturer's instructions.

Stereological methods were used to quantify the number of cells in the peri-infarct areas as described elsewhere.[8] We applied the optical fractionator method to count labeled cells. Peri-infarct regions were outlined at cortical and subcortical levels at $\times 2.5$ magnification on arbitrary uniform random coronal sections, located throughout the entire brain. Individual cells were viewed at $\times 40$ in arbitrary uniform random-sampled sites chosen by the Mercator Pro 7.0 software (ExploraNova, La Rochelle, France) and then counted.

Cell culture and microglial activation

Cell culture procedures were approved by the Ethics Committee of the Universitat de Barcelona, in accordance with the regulations established by the Catalan autonomous government (Generalitat de Catalunya). Primary microglia-enriched cultures were obtained from post-natal day 1 rat brains, following the protocol described by Saura *et al*,[27] with slight modifications. Briefly, mixed glial cultures from post-natal day 1 rat brains were obtained from cerebral cortex and digested with 0.25% trypsin–EDTA solution (Invitrogen) for 30 minutes at 37 °C. Trypsinization was stopped by adding an equal volume of culture medium, consisted in Dulbecco's modified Eagle's medium-F-12 nutrient mixture (DMEM:F12, Invitrogen) supplemented with 10% fetal bovine serum, 0.1% penicillin–streptomycin (Invitrogen), 0.5 μg/mL amphotericin B (Fungizone, Invitrogen), and 0.04% deoxyribonuclease I (Sigma-Aldrich). Cells were pelleted (8 minutes, 1,000 r.p.m.), resuspended in culture medium, and brought to a single-cell suspension by pipetting vigorously and filtering through a 105-μm-pore mesh. Cells suspension were seeded at a density of $3 \cdot 10^5$ cells/mL and grown in a humidifier cell incubator containing 5% CO_2 at 37 °C. Medium was replaced every 7 days. Microglial cultures were prepared by the mild trypsinization method after 19–21 days *in vitro* (DIV), where mixed glial cultures were treated for 30 minutes with 0.06% trypsin–EDTA solution. That resulted in a 97%-enriched microglial culture.

These microglial cultures were activated and treated 24 hours after isolation as described below. Based on our preliminary results, cell cultures were pre-treated with 1 nmol/L glibenclamide diluted in culture medium (dimethyl sulfoxide final concentration $<0.05\%$; Sigma-Aldrich, $>99\%$ purity).[8] Thirty minutes later, cells were activated with 0.1 μg/mL of recombinant lipopolysaccharide (LPS) and 0.05 ng/mL of recombinant mouse interferon gamma (IFNγ; Sigma-Aldrich). After 48 hours, cells were incubated for 30 minutes at 37 °C in Hank's balanced salt solution and supplemented with 500 nmol/L glibenclamide–BODIPY-FL (green fluorescent dye; Invitrogen). After cell fixation with 4% w/v paraformaldehyde, we performed immunocytochemical analyses with mouse antirat CD11b (OX-42 clone; 1:500; Serotec) antibody and goat antimouse AlexaFluor-555 as a secondary antibody (1:500; Molecular Probes, Eugene, OR, USA). Cultures were directly observed in an AxioObserver Z1 (Carl Zeiss, GmbH, Jena, Germany) inverted microscope equipped with FluoUp and CoLoc image software (ExploraNova, Bordeaux, France) and recorded on a high sensitivity camera (RetigaEXi Fast 1394, QImaging, Surrey, BC, Canada). Image processing was performed using the method described by Jaskolski *et al*.[28] The purity of the cultures was $97 \pm 1\%$ ($n = 4$ cultures), as based on the number of CD11b-positive compared with the total number of cell nuclei stained with Hoescht33258 (Invitrogen; 0.1 μg/mL in PBS).

Statistical Analyses

Statgraphics 5.0 (STSC, Rockville, MD, USA) and GraphPad Prism4 (La Jolla, CA, USA) statistical packages were used. *In vitro* and histological data and differences in the infarct volumes between vehicle controls and glibenclamide-treated MCAO rats were analyzed using analysis of variance (ANOVA) followed by *post hoc* test Least Significant Difference. When normality was not reached, we applied the Kruskall–Wallis test followed by the Mann–Whitney *U*-test. Differences in the limb-placing scores between experimental groups were analyzed by the Mann–Whitney *U*-test. We used repeated measures ANOVA to analyze the beam-walking, cylinder, and water-maze data for the overall group effect. Groups were then compared using one-way ANOVA followed by a *post hoc* test Least Significant Difference. Probe trial data were tested by ANOVA followed by Least Significant Difference. All values are presented as mean $\pm$ s.e.m. *P*-values <0.05 were considered significant.

RESULTS

Infarct size, gliosis, neurodegeneration and apoptosis

We analyzed the effects of glibenclamide in terms of lesion volume by histological methods 30 days after MCAO. Quantification of the lesion volume of hematoxylin–eosin-stained sections showed that there was no difference in infarct volume size between vehicle- and glibenclamide-treated MCAO rats (Figure 1A). We then performed stereological quantification of the MCAO-induced neuronal loss in the peri-infarcted volume by NeuN immunohistochemistry. Stereological counting showed same number of NeuN-positive cells in the peri-infarct striatum (Figure 1B), but higher number in the peri-infarct cortex of glibenclamide-treated MCAO rats (Figure 1C, $P<0.05$).

The pattern and cell density of microglia/macrophages (IB4-stained) and astrocytes (GFAP-immunopositive) in ischemic animals showed activation, as evidenced by their reactive morphology (Supplementary Figure 1C). In addition, when we quantified the overall staining and cell density for both markers, we found that glibenclamide did not modify MCAO-induced astrogliosis or microgliosis in the cortex (Supplementary Figure 1A,B).

As hypoxia and ischemia causes neuronal death in the peri-infarcted region, and consequently, secondary neurodegeneration in other brain regions, we analyzed whether neurodegenerative processes were still active 30-days after MCAO by FJB staining. Only scattered FJB-positive neurons were detected in the thalamus (Supplementary Figure 2A). We also studied apoptosis using cleaved caspase-3 immunohistochemistry. Cleaved caspase-3 staining did not co-localize with neurons (NeuN) or astrocytes (GFAP) (Supplementary Figure 2B,C). However, cleaved caspase-3 staining co-localized with some cells expressing the microglial/macrophage marker CD11b in the peri-infarct region (Supplementary Figure 2D). These results suggest that 30-days after ischemia secondary neurodegenerative processes had completed.

Characterization of neuroblast migration and long-term neurogenesis

We hypothesized that glibenclamide treatment could influence neurogenesis after stroke. First, DCX-immunohistochemistry was carried out to detect neuroblasts in the striatum migrating toward the lesion core to a group of rats killed 3 days after MCAO (Sham $n = 3$; MCAO groups $n = 6$). Results showed that sham-operated

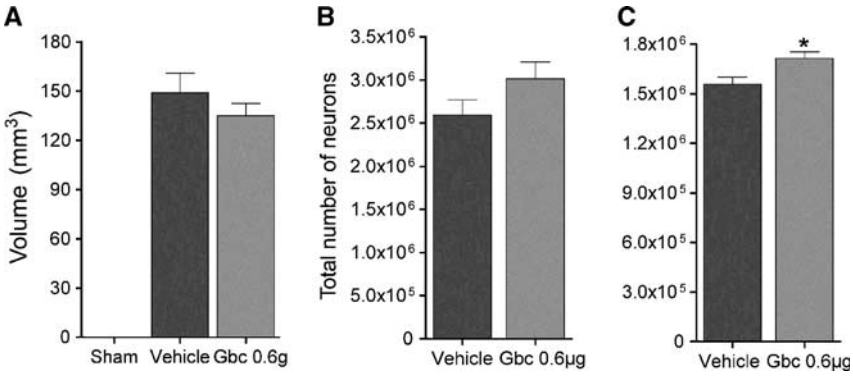

Figure 1. Glibenclamide does not affect corticostriatal infarct size in middle cerebral artery occlusion (MCAO) rats (**A**). Quantification of NeuN-positive cells in the peri-infarct striatum (**B**) and cortex (**C**). Results are mean ± s.e.m. ($n = 10$–12). *$P < 0.05$ (compared with vehicle-treated MCAO rats). Gbc, glibenclamide.

animals had all DCX-positive cells attached to the intact lateral striatum or migrating through the rostral migratory stream (RMS). Contrary, MCAO animals showed increased migration of neural progenitor cells toward the infarct in the striatum (Figure 2A,B) as reported previously.[13,22] Interestingly, we found more migrating neuroblasts in the striatum of glibenclamide-treated than in vehicle-treated MCAO rats ($P < 0.001$, Figure 2A,B). Neuroblast migration toward the infarct core in the striatum was still active 30 days after MCAO (Figure 2C,D) and the migration pattern was not altered by glibenclamide administration. In line, microglia from the medial striatum became reactive after ischemia, but we did not observe a change in their morphology driven by glibenclamide treatment (Figure 2A).

Second, to detect cell proliferation, we perfused a group of rats 30 days after MCAO (sham $n = 9$, vehicle $n = 10$, and glibenclamide-treated group $n = 12$). Immunohistochemistry against BrdU showed that vehicle-treated MCAO rats had more BrdU-positive cells in the cerebral cortex ($P < 0.001$) than sham-operated rats (Figure 3A). Glibenclamide treatment increased the number of BrdU-positive cells in the cerebral cortex ($P < 0.001$) and in the CA1 pyramidal layer ($P < 0.05$; glibenclamide vs. sham) (Figure 3A). Then, using the same group of animals, we performed double immunohistochemistries to identify the cell lineage of proliferative cells (Figure 3A,B). Quantitative results showed an increased number BrdU/NeuN-positive cells in the cerebral cortex in vehicle-treated MCAO rats ($P < 0.001$) and this was further boosted by glibenclamide treatment ($P < 0.001$; glibenclamide- vs. vehicle-treated MCAO rats). A slight increase in the number of BrdU/NeuN-positive cells was found in the CA1 region and in the subgranular zone of the hippocampus ($P < 0.05$; glibenclamide vs. sham), although this increase was not statistically significant compared with the vehicle group. In addition, the other neuronal population markers (e.g., parvalbumin, tyrosine hydroxylase, and calbindin) were also analyzed, but did not co-localize with BrdU (data not shown). The number of BrdU/GFAP-positive cells increased in the cortex of vehicle-treated MCAO rats ($P < 0.001$) (Figure 3A,B), pointing to an astroglial proliferation caused by the lesion. Also in the cortex, glibenclamide-treated MCAO rats showed increased astroglial proliferation ($P < 0.001$) compared with sham-operated rats and vehicle-treated MCAO rats. We then analyzed macrophages/microglia proliferation, and we observed an increased number of BrdU/IB4-stained cells in the cortex ($P < 0.001$) and in the CA1 pyramidal layer ($P < 0.001$) of MCAO rats (Figure 3A,B).

To study whether glibenclamide modifies the fate of the neuroblasts as they migrate through the RMS, we quantified the number of BrdU-positive cells in the olfactory bulb 30 days after MCAO. No differences in the number of these cells were found between MCAO groups in the olfactory bulb (542 ± 26 BrdU-positive cells/section for sham-operated, 518 ± 37 for vehicle-treated group and 580 ± 28 for glibenclamide-treated group). As the total number of proliferative cells in the olfactory bulb is not modified by ischemia or glibenclamide, the most likely the fate of neuroblasts migrating through the RMS is also unaffected. Therefore, these results indicate that glibenclamide strengthens intrinsic neurogenic processes as higher numbers of NeuN/BrdU-positive cells were found in the cortex.

Angiogenesis

To assess another brain repair mechanism, we studied angiogenesis in several brain regions by measuring vessel diameter and RECA-1 immunoreactivity 30 days after ischemia.[29] The diameter of vessels increased in the ipsilateral cortex of glibenclamide-treated MCAO rats (Figure 4A,C). Quantitative analysis of RECA-1 immunoreactivity showed increased microvessel density in the ipsilateral hippocampus of glibenclamide-treated MCAO rats (Figure 4B,C; $P < 0.01$). This difference was not detected in the peri-infarct cortex, although a slight increase was found.

Recovery of sensorimotor and cognitive functions

The effects of ischemia and glibenclamide treatment in the recovery of sensorimotor and cognitive functions were analyzed using a battery of behavioral tests during a 30-day follow-up period. Spontaneous forelimb use was analyzed by the cylinder test (Figure 5A). Analysis of variance for repeated measures showed an overall group effect ($P < 0.05$), but no significant group × time interaction, thereby indicating that forelimb use differed between groups. A *post hoc* analysis revealed that forelimb use between sham-operated and vehicle-treated MCAO rats was different ($P < 0.05$), but not between sham-operated and glibenclamide-treated MCAO rats. Forelimb use in the MCAO groups was different from that in sham-operated rats on postoperative day 7 ($P < 0.01$). Impaired forelimb use in MCAO rats treated with glibenclamide was recovered and these animals showed similar performance to that of sham-operated rats at the end of the follow-up period.

We then used the limb-placing test to further analyze recovery of the forelimb function. All ischemic animals presented initial severe impairment in the limb-placing test after MCAO, followed by spontaneous recovery during the follow-up (Figure 5B). Limb-placing scores between sham-operated and MCAO rats were different in all post-operative time points ($P < 0.01$). MCAO rats treated with glibenclamide showed an improved score compared with the vehicle group on postoperative days 22 to 29 ($P < 0.05$; $P < 0.01$).

The effect of glibenclamide on recovery of hindlimb function in MCAO rats was analyzed by tapered/ledged beam walking.

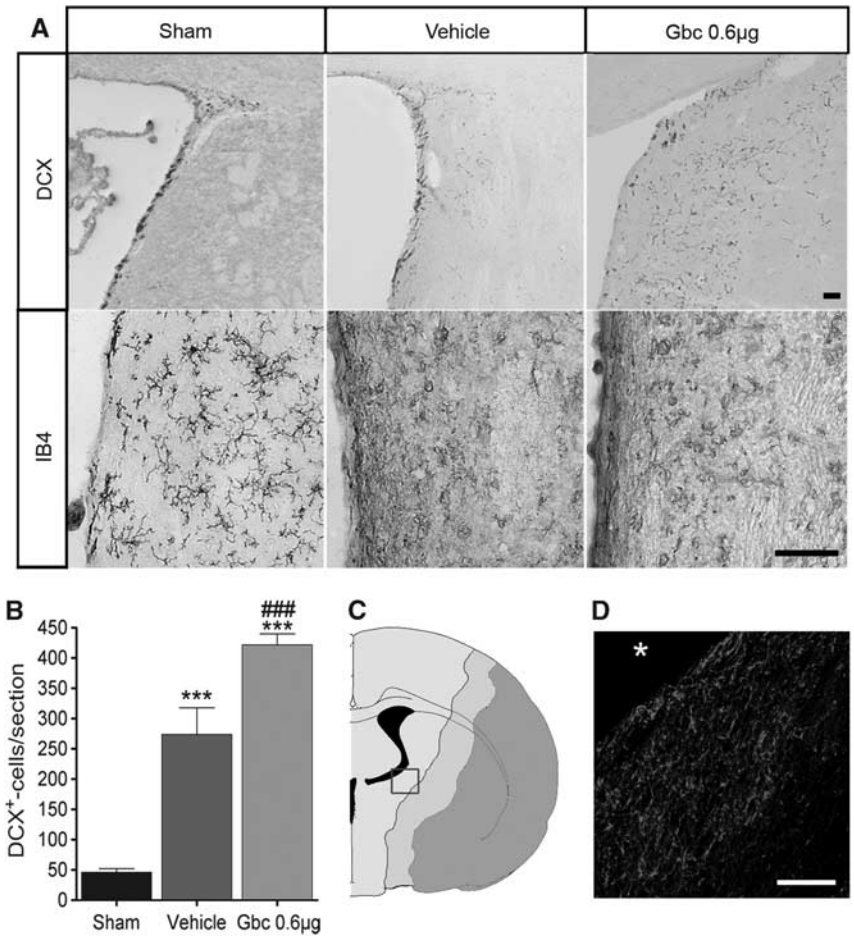

Figure 2. Glibenclamide (Gbc) enhances neuroblast migration toward the ischemic lesion. Representative micrographs of doublecortin (DCX) and microglia/macrophage (IB4) immunostaining in the striatum adjacent to the ventricle of sham-operated rat and vehicle- and Gbc- (0.6 μg) treated middle cerebral artery occlusion (MCAO) rats 3 days after ischemia (**A**). Quantitative analysis of the migrating neuroblasts/section toward the striatal lesion (**B**). Coronal section representation of an ischemic rat brain (bregma -0.8), where dark pink denotes for the necrotic core, light pink for peri-infarct area, and green for healthy tissue (**C**). Enlarged image of the blue box from the left, in which DCX-positive cells (red) were still present in the peri-infarct striatum 30 days after MCAO (asterisk denotes the striatal lesion core) (**D**). Results are mean $\pm$ s.e.m. ($n = 3$–6). $^{***}P < 0.001$ (compared with sham rats); $^{\#\#\#}P < 0.001$ (compared with vehicle-treated MCAO rats). Bar $= 50\ \mu$m.

Analysis of variance for repeated measures showed an overall group effect ($P < 0.01$) and a group $\times$ day interaction ($P < 0.01$). However, there was no difference between glibenclamide-treated and vehicle-treated MCAO rats ($P = 0.81$) (data not shown).

Results from the Morris water-maze on post-operative days 26 to 28 showed that escape latency, length and swimming speed did not differ between groups. No significant differences were observed in the number of passes over the removed platform or the time rats spent in the target quadrant (probe trial). However, a thigmotaxis behavior was observed in vehicle-treated MCAO rats, which they spent more time in the outermost zone (zone 3; $P < 0.05$) and less time in the middle zone (zone 2; $P < 0.01$) compared with sham-operated animals (Figure 5C,D). The search strategy in glibenclamide-treated MCAO rats was similar to that of sham-operated animals.

Glibenclamide binds to reactive microglia

To assess whether microglia express the K_{ATP}-channel components after ischemia, we performed double immunohistochemical labeling against SUR1 and Kir6.2 combined with the microglia/macrophage marker CD11b. Co-location of striatal CD11b-positive cells adjacent to the ventricle indicated that the reactive microglia of MCAO animals expressed the K_{ATP}-channel components SUR1 and Kir6.2 at 72 hours after ischemia (Figure 6A). To determine the specificity of binding to SUR1 expressed by microglia, we analyzed the binding of fluorescently tagged glibenclamide (glibenclamide BODIPY FL; green fluorescence) in primary rat microglial cultures. When microglial cells were in the resting state, glibenclamide labeling was localized to the perinuclear space (Figure 6B). Forty-eight hours after LPS + IFNγ activation, glibenclamide labeling was present in the plasmalemmal membrane, denoting a translocation of SUR1 from its internal reservoir toward the cell surface.

DISCUSSION

Previous preclinical and clinical data suggest a neuroprotective role for glibenclamide after cerebral ischemia.[3,4] Here we showed that glibenclamide also enhanced early migration of neuroblasts toward the striatal lesion core and facilitated long-term brain repair in MCAO rats. Interestingly, this was associated with improved behavioral recovery.

After a stroke, massive necrotic or apoptotic processes are activated in the ischemic core, as well as in distal regions owing to Wallerian neurodegeneration. In our model, we only observed a few scattered FJB-positive neurodegenerative cells, which were mainly located in the thalamus 30-days after ischemia.

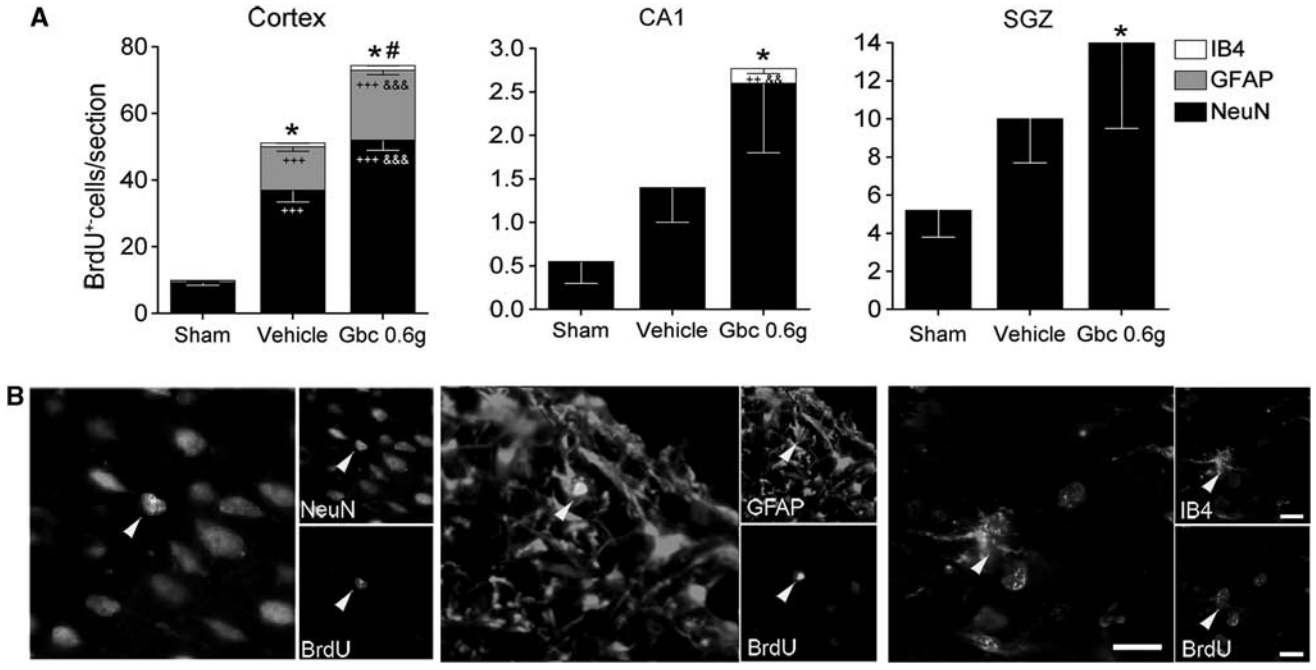

Figure 3. Characterization of proliferative cells into the ischemic brain. Quantitative analysis of the total number of 5-bromo-2-deoxyuridine (BrdU)-positive cells/section and relative number of neurons (NeuN), astrocytes (GFAP), and microglia (IB4) double-stained BrdU-positive cells in the cortex, CA1 pyramidal cell layer, and subgranular zone (SGZ) (**A**). Confocal photomicrographs of the rat cortex showing colocalization of BrdU (in green) with NeuN, GFAP, and IB4 (red) (**B**). Glibenclamide (Gbc) increased the total number of BrdU-positive cells after middle cerebral artery occlusion (MCAO). These cells preferentially co-localized with markers of neurons and astrocytes. Bar 10 μm. Results are mean ± s.e.m. ($n = 9$–10). $^{*}P < 0.05$ (total BrdU-positive cells compared with sham-operated rats); $^{\#}P < 0.05$ (total BrdU-positive cells compared with vehicle-treated MCAO rats); $^{++}P < 0.01$, $^{+++}P < 0.001$ (cell type compared with sham-operated rats); $^{\&\&}P < 0.01$, $^{\&\&\&}P < 0.001$ (cell type compared with vehicle-treated MCAO rats).

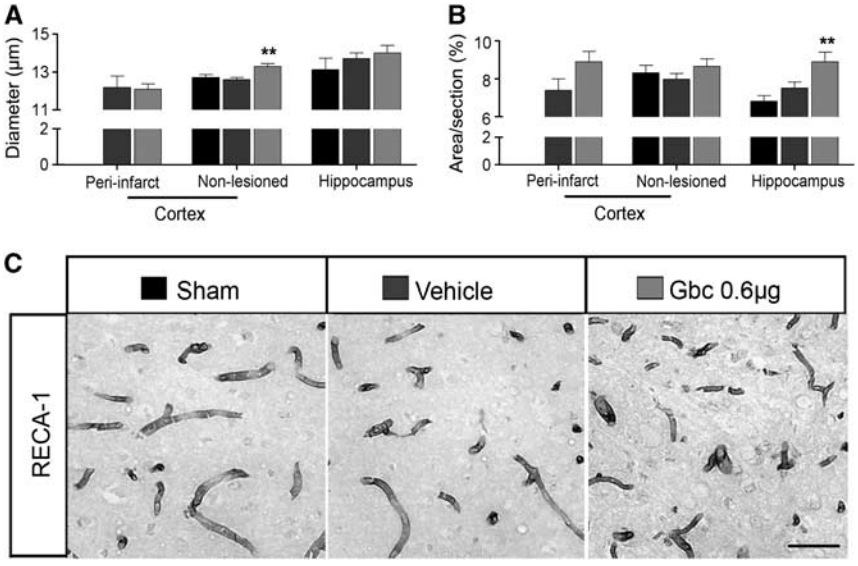

Figure 4. Glibenclamide (Gbc) fosters angiogenesis in the cortex and hippocampus of ischemic animals. Quantitative analysis of the microvessel diameter (**A**) and RECA-1 immunoreactivity (**B**) in the cortex and hippocampus after middle cerebral artery occlusion (MCAO). Gbc administration increased microvessel diameter in the non-lesioned cortex and RECA-1 immunoreactivity in the hippocampus. Representative micrographs of RECA-1 immunoreactive microvessels in the cortex of sham-operated rat, vehicle- and Gbc-treated (0.6 μg) MCAO rats (**C**). Bar 50 μm. Results are mean ± s.e.m. ($n = 6$–11). $^{**}P < 0.01$ (compared with sham-operated and vehicle-treated MCAO rats).

In addition, the only cells labeled by cleaved caspase-3 in the peri-infarct zone were some microglia/macrophages. Recent data demonstrated that cleaved caspase-3, a known mediator of apoptosis, regulates microglial activation by a non-apoptotic pathway.[30] Thus, we here found that 30-days after ischemia the majority of secondary neurodegenerative processes have been completed and caspase-3-positive microglia/macrophages may be participating in the tissue repair response to injury instead of undergoing apoptosis. Although glibenclamide did not reduce the size of the infarct, our results are in line with Simard *et al*,[10]

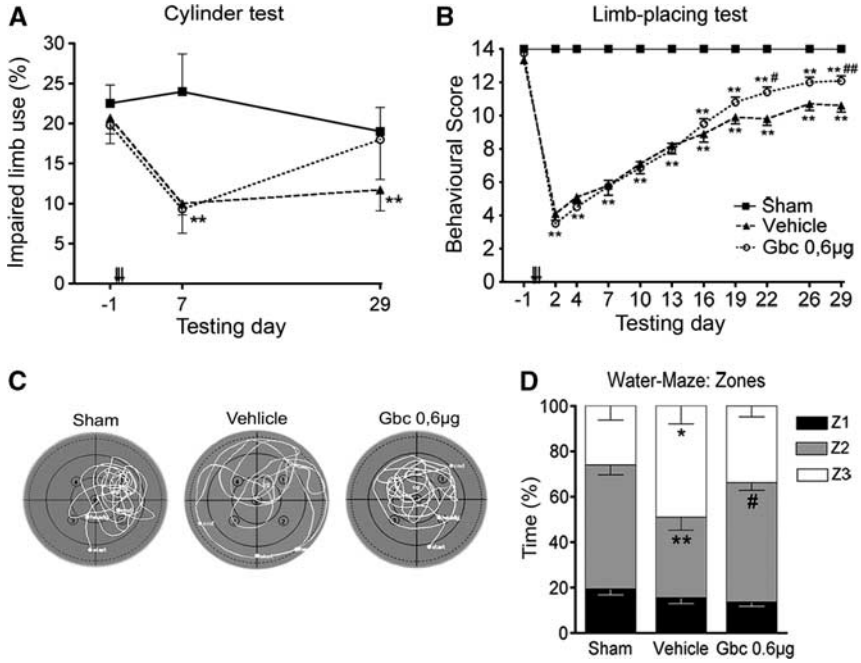

Figure 5. Ischemic animals showed long-term improvement of neurological function after glibenclamide (Gbc) treatment. Contralateral forelimb use (cylinder test) (**A**) and limb-placing scores (**B**) during a 30-day follow-up after middle cerebral artery occlusion (MCAO). Swimming strategy in the probe trial test (Morris water-maze) on post-operative day 28 (**C, D**). Here the values are shown as a percentage of time spent in equal zones of the pool. Zone 1 refers to the inner annulus and zone 3 the outermost annulus. Results are mean ± s.e.m. ($n = 9$–12). $^{*}P < 0.05$; $^{**}P < 0.01$ (compared with sham-operated rats); $^{\#}P < 0.05$; $^{\#\#}P < 0.01$ (compared with vehicle-treated MCAO rats).

confirming that some factor other than infarct volume determined the long-term functional recovery outcome. Interestingly, in the Morris water-maze task, we observed thigmotaxis behavior in vehicle-treated MCAO animals (i.e., swimming close to the walls of the tank), which was decreased after glibenclamide treatment. However, whether thigmotaxis is related to cognitive or noncognitive strategies, or hippocampus-derived increases in stress or anxiety, still remain open.[31,32] Thus, from our data we cannot rule out the possibility that glibenclamide, instead of improving cognitive outcome, ameliorates stress or anxiety caused by ischemia. It is noteworthy to mention here that our approach for glibenclamide administration is different to that used by Simard *et al*,[3,7,10] who administered an intraperitoneal loading dose of 10 μg/kg plus a subcutaneous infusion dose of 200 ng/hour using an osmotic mini-pump. We administered glibenclamide intravenously with 3 doses of 0.2 μg beginning 6 hours after onset of ischemia. The facts that the subunit SUR1 has a particularly high affinity for glibenclamide,[33] the ischemic brain shows preferential uptake for glibenclamide,[7,8] and that we here use intravenous glibenclamide administration instead of subcutaneous infusion could explain our results. However, the dose of glibenclamide was lower than the doses used in previous studies.

Focal cerebral ischemia promotes neurogenesis in the subventricular zone and the subgranular zone of the dentate gyrus and induces neuroblast migration toward the striatal ischemic boundary.[13,22] Recent data have provided new evidence that the cerebral cortex also has the same capacity[17] and, more importantly, stroke-induced cortical neurogenesis has also been found in the adult human brain.[19,20] In the present study, ischemia increased neuroblast migration toward the lesion 3 days after ischemia/reperfusion and this event persisted for up to 1 month. Inhibition of SUR1 using glibenclamide led to a further increase in the number of migrating neuroblasts, thereby indicating that glibenclamide modifies the cell lineage choice or enhances progenitor cell proliferation and migration.

Proliferative cells detected by administration of BrdU from days 4 to 8 after ischemia/reperfusion showed increased co-expression of NeuN in the peri-infarct area of the cortex 30 days after reperfusion and this was potentiated by glibenclamide. Although we cannot exclude the possibility that some neural progenitors migrate from the subventricular zone to establish themselves in the ipsilateral cortical network, we found no co-localization of BrdU-positive cells with the classical RMS-derived neuronal markers (i.e., calbindin, calretinin, tyrosine hydroxylase, and parvalbumin) and no change in the total number of proliferative cells in the olfactory bulb. Thus, these newborn cortical neurons may have originated from potential resident neural stem cells within the cortex.[17] Several authors have proposed that these endogenous quiescent neural stem cells are present in the cerebral cortex and that their proliferation and differentiation to mature neurons is induced by ischemic insults.[18] Although the number of these cells may be small, strategies to foster their intrinsic neurogenic potential would be highly relevant for clinical approaches to facilitate neural repair and functional recovery.

Another purpose of this study was to investigate angiogenesis after cerebral infarction, because angiogenesis is also activated after cerebral ischemia. Generally, tissue repair is activated at 2 to 3 days after reperfusion, and the infarction is eventually encircled by a glial scar a few weeks later. As the glial response, in terms of the reactive area or cell density, was not modified by glibenclamide, we analyzed the microvessel diameter and the surface density as a parameter to quantify angiogenesis.[29] We herein demonstrated that glibenclamide causes microvascular changes, where interestingly, glibenclamide further increased the diameter of microvessels in the non-lesioned cortex and RECA-1 immunoreactivity in the hippocampus, and both regions showed glial proliferation. These observations are consistent with those of Fantin *et al*,[34] who reported that tissue macrophages/microglia are associated with angiogenesis in various developing organs. Vasculature attracts microglial cells and stimulates them to release angiogenic factors,[35] with subsequent growth stimulation

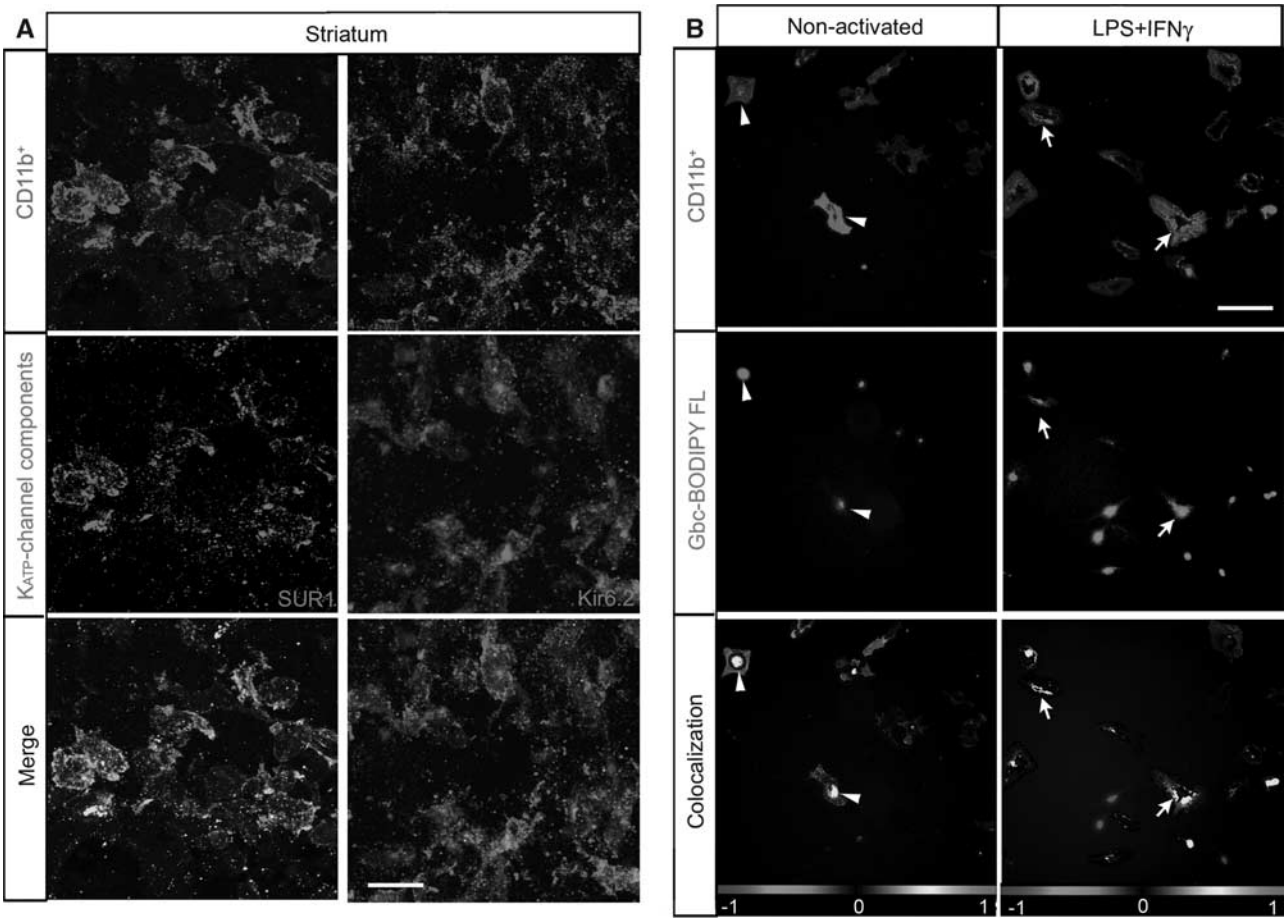

Figure 6. Reactive microglia express and translocate sulfonylurea receptor 1 (SUR1) to the cell surface. (**A**) Confocal photomicrographs of SUR1 and Kir6.2 (green) in reactive microglia (CD11b-positive; red) localized to the medial striatum in middle cerebral artery occlusion rats. Yellow in the merge image denotes colocalization, whereby reactive CD11b-postive cells expressed SUR1 or Kir6.2 72 hours after ischemia. (**B**) Localization of glibenclamide (Gbc) (Gbc BODIPY FL; green fluorescence) in rat microglial primary culture. Non-activated or cultures activated with lipopolysaccharide (LPS) + interferon gamma (IFNγ) for 48 hours are shown in the upper row. Microglial cells were labeled with an anti-CD11b (red) antibody and Hoechst (blue) to stain the nuclei. Lower row shows respective colocalization of the red and green channels, where the yellow denotes the presence of the Gbc binding in microglial cells. Arrowhead denotes perinuclear colocalization and arrows show surface labeling. The data shown are representative of four experiments each. Scale bar in (**A**) is 15 μm and in (**B**) is 20 μm.

of neural stem cells.[36] Furthermore, angiogenesis is considered a key feature of ischemic stroke recovery and neuronal post-stroke re-organization.[37]

Several studies using experimental stroke models have indicated the beneficial effects of glibenclamide administration after reperfusion, such as reversing ischemia-reperfusion injury by halting oxidative stress and inflammation in the hippocampus,[9] preventing cytotoxic edema after cerebral ischemia,[2,3,1,7] and enhancing neuroprotection, which all eventually lead to a better functional outcome.[8] Thus, although glibenclamide did not modify the size and cell density of microglia nor astroglia after ischemia here, it enhanced long-term brain repair processes and functional recovery outcomes of the rats. We recently reported that 72 hours after MCAO, activated microglia/macrophages in the ischemic hemisphere increase K_{ATP}-channel expression, and so does the murine microglial BV2 cell line 48 hours after inflammatory stimuli.[8] We have now confirmed these results in postnatal primary rat microglial cultures. When microglial cells became activated after pro-inflammatory stimuli, they showed higher specific glibenclamide labeling and the signal extended to the plasmalemmal membrane *in vitro*, pointing toward a mobilization of SUR1 from its internal reservoir in the endoplasmic reticulum and Golgi apparatus, toward the cell surface. Also, reactive microglia located in the lateral striatum 72 hours after MCAO expressed the K_{ATP}-channel components SUR1 and Kir6.2. All these results suggest that after microglial activation, K_{ATP}-channel expression is increased and the channel becomes translocated to the cell surface where it can exert its function in brain pathologies. *In vitro* glibenclamide regulates microglial phagocytic activity and the release of cytokines/chemokines after pro-inflammatory stimuli.[8,11] As postnatal and adult microglia constitutively express low levels of SUR1,[8,11,12] it is likely that regardless of the age of the animal the expression of SUR1 is upregulated by cell death/damage signals. Nonetheless, although glibenclamide possibly also blocks the SUR1 subunits of K_{ATP} or $NC_{Ca\text{-}ATP}$ channels expressed in neurons, astrocytes, and capillary endothelial cells,[2,3] there is increasing evidence that microglia participate in modifications of stem cell proliferation, migration, and/or differentiation by producing trophic factors and inflammatory cytokines/chemokines.[15,16] Thus, as microglial activation is a dynamic and complex process,[38] the pro- or antineurogenic niche would depend on the degree of microglial activation and the balance between the pro- and anti-inflammatory soluble cytokines produced, without cell–cell contact required to direct this effect.[16,21] In this scenario, it is possible that the interaction of glibenclamide with SUR1 endows microglia

from the lateral striatum to carry a distinct phenotype that releases soluble factors with paracrine effects, which consequently enhance neurogenesis and the migration of neuroblasts toward the lesion.

In summary, we have demonstrated here that early blockade of SUR1 by glibenclamide produces long-term cortical neuroprotection, stimulates neuroblast migration toward the striatal lesion, and strengthens neurogenesis in the cortex after cerebral ischemia. All these results were temporally associated with improved long-term behavioral recovery. Therefore, these data identify SUR1 as a multifaceted target that promotes both long-term neuroprotective processes and brain repair mechanisms. Further experiments are necessary to identify the specific role of the microglial K_{ATP} channel and its diffusible mediators that may modulate brain repair, which will help us to shed light on the understanding of the intricate mechanisms underlying neurogenesis and neuroprotection after stroke caused by glibenclamide treatment.

DISCLOSURE/CONFLICT OF INTEREST

NM and MJR hold an EU patent (No. WO2006/000608). The other authors report no disclosures.

REFERENCES

1 Simard JM, Woo SK, Schwartzbauer GT, Gerzanich V. Sulfonylurea receptor 1 in central nervous system injury: a focused review. *J Cereb Blood Flow Metab* 2012; **32**: 1699–1717.
2 Simard JM, Tsymbalyuk N, Tsymbalyuk O, Ivanova S, Yurovsky V, Gerzanich V. Glibenclamide is superior to decompressive craniectomy in a rat model of malignant stroke. *Stroke* 2010; **41**: 531–537.
3 Simard JM, Yurovsky V, Tsymbalyuk N, Melnichenko L, Ivanova S, Gerzanich V. Protective effect of delayed treatment with low-dose glibenclamide in three models of ischemic stroke. *Stroke* 2009; **40**: 604–609.
4 Kunte H, Schmidt S, Eliasziw M, del Zoppo GJ, Simard JM, Masuhr F *et al.* Sulfonylureas improve outcome in patients with type 2 diabetes and acute ischemic stroke. *Stroke* 2007; **38**: 2526–2530.
5 Mikhailov MV, Campbell JD, De Wet H, Shimomura K, Zadek B, Collins RF *et al.* 3-D structural and functional characterization of the purified K_{ATP} channel complex Kir6.2-SUR1. *EMBO J* 2005; **24**: 4166–4175.
6 Chen M, Simard JM. Cell swelling and a nonselective cation channel regulated by internal Ca^{2+} and ATP in native reactive astrocytes from adult rat brain. *J Neurosci* 2001; **21**: 6512–6521.
7 Simard JM, Chen M, Tarasov KV, Bhatta S, Ivanova S, Melnitchenko L *et al.* Newly expressed SUR1-regulated $NC_{Ca\text{-}ATP}$ channel mediates cerebral edema after ischemic stroke. *Nat Med* 2006; **12**: 433–440.
8 Ortega FJ, Gimeno-Bayon J, Espinosa-Parrilla JF, Carrasco JL, Batlle M, Pugliese M *et al.* ATP-dependent potassium channel blockade strengthens microglial neuroprotection after hypoxia-ischemia in rats. *Exp Neurol* 2012; **235**: 282–296.
9 Abdallah DM, Nassar NN, Abd-El-Salam RM. Glibenclamide ameliorates ischemia-reperfusion injury via modulating oxidative stress and inflammatory mediators in the rat hippocampus. *Brain Res* 2011; **1385**: 257–262.
10 Simard JM, Woo SK, Tsymbalyuk N, Voloshyn O, Yurovsky V, Ivanova S *et al.* Glibenclamide-10-h treatment window in a clinically relevant model of stroke. *Transl Stroke Res* 2012; **3**: 286–295.
11 Virgili N, Espinosa-Parrilla JF, Mancera P, Pastén-Zamorano A, Gimeno-Bayon J, Rodríguez MJ *et al.* Oral administration of the K_{ATP} channel opener diazoxide ameliorates disease progression in a murine model of multiple sclerosis. *J Neuroinflammation* 2011; **8**: 149.
12 Ramonet D, Rodriguez MJ, Pugliese M, Mahy N. Putative glucosensing property in rat and human activated microglia. *Neurobiol Dis* 2004; **17**: 1–9.
13 Thored P, Heldmann U, Gomes-Leal W, Gisler R, Darsalia V, Taneera J *et al.* Long-term accumulation of microglia with proneurogenic phenotype concomitant with persistent neurogenesis in adult subventricular zone after stroke. *Glia* 2009; **57**: 835–849.
14 Carson MJ, Doose JM, Melchior B, Schmid CD, Ploix CC. CNS immune privilege: hiding in plain sight. *Immunol Rev* 2006; **213**: 48–65.
15 Ekdahl CT, Kokaia Z, Lindvall O. Brain inflammation and adult neurogenesis: the dual role of microglia. *Neuroscience* 2009; **158**: 1021–1029.
16 Butovsky O, Ziv Y, Schwartz A, Landa G, Talpalar AE, Pluchino S *et al.* Microglia activated by IL-4 or IFN-gamma differentially induce neurogenesis and oligodendrogenesis from adult stem/progenitor cells. *Mol Cell Neurosci* 2006; **31**: 149–160.
17 Shimada IS, Peterson BM, Spees JL. Isolation of locally derived stem/progenitor cells from the peri-infarct area that do not migrate from the lateral ventricle after cortical stroke. *Stroke* 2010; **41**: e552–e560.
18 Jiang W, Gu W, Brannstrom T, Rosqvist R, Wester P. Cortical neurogenesis in adult rats after transient middle cerebral artery occlusion. *Stroke* 2001; **32**: 1201–1207.
19 Macas J, Nern C, Plate KH, Momma S. Increased generation of neuronal progenitors after ischemic injury in the aged adult human forebrain. *J Neurosci* 2006; **26**: 13114–13119.
20 Jin K, Wang X, Xie L, Mao XO, Zhu W, Wang Y *et al.* Evidence for stroke-induced neurogenesis in the human brain. *Proc Natl Acad Sci USA* 2006; **103**: 13198–13202.
21 Walton NM, Sutter BM, Laywell ED, Levkoff LH, Kearns SM, Marshall GP *et al.* Microglia instruct subventricular zone neurogenesis. *Glia* 2006; **54**: 815–825.
22 Arvidsson A, Collin T, Kirik D, Kokaia Z, Lindvall O. Neuronal replacement from endogenous precursors in the adult brain after stroke. *Nat Med* 2002; **8**: 963–970.
23 Puurunen K, Jolkkonen J, Sirviö J, Haapalinna A, Sivenius J. An alpha(2)-adrenergic antagonist, atipamezole, facilitates behavioral recovery after focal cerebral ischemia in rats. *Neuropharmacology* 2001; **40**: 597–606.
24 Karhunen H, Virtanen T, Schallert T, Sivenius J, Jolkkonen J. Forelimb use after focal cerebral ischemia in rats treated with an α2-adrenoceptor antagonist. *Pharmacol Biochem Behav* 2003; **74**: 663–669.
25 Zhao C-S, Puurunen K, Schallert T, Sivenius J, Jolkkonen J. Effect of cholinergic medication, before and after focal photothrombotic ischemic cortical injury, on histological and functional outcome in aged and young adult rats. *Behav Brain Res* 2005; **156**: 85–94.
26 Valente T, Hidalgo J, Bolea I, Ramirez B, Anglés N, Reguant J *et al.* A diet enriched in polyphenols and polyunsaturated fatty acids, LMN diet, induces neurogenesis in the subventricular zone and hippocampus of adult mouse brain. *J Alzheimers Dis* 2009; **18**: 849–865.
27 Saura J, Tusell JM, Serratosa J. High-yield isolation of murine microglia by mild trypsinization. *Glia* 2003; **44**: 183–189.
28 Jaskolski F, Mulle C, Manzoni OJ. An automated method to quantify and visualize colocalized fluorescent signals. *J Neurosci Methods* 2005; **146**: 42–49.
29 Czéh B, Abumaria N, Rygula R, Fuchs E. Quantitative changes in hippocampal microvasculature of chronically stressed rats: no effect of fluoxetine treatment. *Hippocampus* 2010; **20**: 174–185.
30 Burguillos MA, Deierborg T, Kavanagh E, Persson A, Hajji N, Garcia-Quintanilla A *et al.* Caspase signalling controls microglia activation and neurotoxicity. *Nature* 2011, 1–7.
31 Goss CW, Hoffman SW, Stein DG. Behavioral effects and anatomic correlates after brain injury: a progesterone dose-response study. *Pharmacol Biochem Behav* 2003; **76**: 231–242.
32 Mendez IA, Montgomery KS, LaSarge CL, Simon NW, Bizon JL, Setlow B. Long-term effects of prior cocaine exposure on morris water maze performance. *Neurobiol Learn Mem* 2008; **89**: 185–191.
33 Dörschner H, Brekardin E, Uhde I, Schwanstecher C, Schwanstecher M. Stoichiometry of sulfonylurea-induced ATP-sensitive potassium channel closure. *Mol Pharmacol* 1999; **55**: 1060–1066.
34 Fantin A, Vieira JM, Gestri G, Denti L, Schwarz Q, Prykhozhij S *et al.* Tissue macrophages act as cellular chaperones for vascular anastomosis downstream of VEGF-mediated endothelial tip cell induction. *Blood* 2010; **116**: 829–840.
35 Rymo SF, Gerhardt H, Wolfhagen Sand F, Lang R, Uv A, Betsholtz C. A two-way communication between microglial cells and angiogenic sprouts regulates angiogenesis in aortic ring cultures. *PLoS ONE* 2011; **6**: e15846.
36 Androutsellis-Theotokis A, Rueger MA, Park DM, Boyd JD, Padmanabhan R, Campanati L *et al.* Angiogenic factors stimulate growth of adult neural stem cells. *PLoS ONE* 2010; **5**: e9414.
37 Slevin M, Kumar P, Gaffney J, Kumar S, Krupinski J. Can angiogenesis be exploited to improve stroke outcome? Mechanisms and therapeutic potential. *Clin Sci* 2006; **111**: 171–183.
38 Schwartz M, Butovsky O, BrÅck W, Hanisch UK. Microglial phenotype: is the commitment reversible? *Trends Neurosci* 2006; **29**: 68–74.

Supplementary Information accompanies the paper on the Journal of Cerebral Blood Flow & Metabolism website (http://www.nature.com/jcbfm)